ORIGINAL ARTICLE

The role of in-situ ocean data assimilation in ECMWF subseasonal forecasts of SST and MLD over the tropical Pacific Ocean

Ho-Hsuan Wei[1,2*] | **Aneesh C. Subramanian**[1] | **Kristopher B. Karnauskas**[1,2] | **Danni Du**[1] | **Magdalena A. Balmaseda**[3] | **Beena B. Sarojini**[3] | **Frederic Vitart**[3] | **Charlotte A. DeMott**[4] | **Matthew R. Mazloff**[5]

[1]University of Colorado, Boulder, Colorado, USA

[2]Cooperative Institute for Research in Environmental Sciences, Boulder, Colorado, USA

[3]The European Centre for Medium-Range Weather Forecasts, Reading, UK

[4]Colorado State University, Fort Collins, Colorado, USA

[5]Scripps Institution of Oceanography, University of California San Diego, La Jolla, California, USA

Correspondence
Ho-Hsuan Wei, University of Colorado and Cooperative Institute for Research in Environmental Sciences, Boulder, Colorado, USA
Email: hohsuan.wei@colorado.edu

Funding information
NOAA, Grant/Award Number: NA18OAR4310405 and NA18OAR4310406; CIRES Visiting Fellowship

The tropical Pacific plays an important role in modulating the global climate through its prevailing sea surface temperature spatial structure and dominant climate modes like ENSO, MJO, and their teleconnections. These modes of variability, including their oceanic anomalies, are considered to provide sources of prediction skill on subseasonal timescales in the tropics. Therefore, this study aims to examine how assimilating in-situ ocean observations influences the initial ocean sea surface temperature (SST) and mixed layer depth (MLD) and their subseasonal forecasts. We analyze two subseasonal forecast systems generated with European Centre for Medium-Range Weather Forecasts (ECMWF) Integrated Forecast System (IFS) where the ocean states were initialized using two Observing System Experiment (OSE) reanalyses. We find that the SST differences between forecasts with and without ocean data assimilation grow with time, resulting in a reduced cold tongue bias when assimilating ocean observations. Two mechanisms related to air-sea coupling are considered to contribute to this growth of SST

* current affiliation: CIRES/NOAA PSL

differences. One is a positive feedback between zonal SST gradient, pressure gradient, and surface wind. The other is the difference in Ekman suction and mixing at the equator due to surface wind speed differences. While the initial mixed layer depth (MLD) can be improved through ocean data assimilation, this improvement is not maintained in the forecasts. Instead, the MLD in both experiments rapidly shoals at the beginning of the forecast. These results emphasize how initialization and model biases influence the air-sea interaction and the accuracy of subseasonal forecast in the tropical Pacific.

KEYWORDS
Observing System Experiment (OSE), ocean initialization, ocean in-situ observations, data assimilation, subseasonal forecast, tropical Pacific, predictability

1 | INTRODUCTION

Through variations in the prevailing pattern of the warm pool in the western Pacific and the cold tongue in the eastern Pacific, the tropical Pacific region exerts its influence on global climate systems through dominant climate modes, including El Niño-Southern Oscillation (ENSO) on the interannual time scale, the Madden-Julian Oscillation (MJO) on subseasonal timescale, and their teleconnections through heating of the lower troposphere and resulting anomalous circulations. The air-sea interaction processes, which are related to the exchanges of heat, freshwater, momentum, and gases across the air-sea interface, can influence both the oceanic and atmospheric processes within climate systems on different timescales.

The subsurface ocean structure, especially density stratification, which can be quantified by the mixed layer depth (MLD), can influence the ocean's response to different forcings and thus is important for air-sea interaction processes. For instance, a shallower MLD (i.e., the density stratified at a shallower level) is more sensitive to surface forcings of momentum (e.g., wind stress) and heat (e.g., surface heat fluxes, and cooling due to vertical mixing and entrainment). A shallower MLD is also subject to greater solar penetration at the bottom of the mixed layer, which would reduce the absorption of heat by the mixed layer. These processes will therefore influence the response of the sea surface temperature (SST) through air-sea interaction processes (e.g. Shi et al., 2022). In addition to the MLD, the thermohaline structure of the upper ocean can also be characterized by the isothermal layer depth (ILD) and the barrier layer thickness (defined as the difference between ILD and MLD), which are known to be important for the air-sea interaction as well (e.g. Lukas and Lindstrom, 1991; Sprintall and Tomczak, 1992; Maes et al., 2002; Wei et al., 2021). These studies suggest that an adequate representation of the ocean subsurface structure, for both temperature and salinity, is important for air-sea interaction processes and can influence the climate systems locally and remotely, and across a range of timescales. The representation of these ocean states in forecast models and their feedback to the atmosphere suggest that biases in the initialization and evolution of ocean states can affect forecast skill for lead times longer than about two weeks (i.e., beyond the atmosphere's dependence on the atmospheric initial state).

In forecasts (or reforecasts), model states are constrained by a relatively realistic initial condition and evolve toward the states closer to the model climatological states (e.g. Ma et al., 2014). The drift to the model climatological state depends on the model initialization, model biases, and the variable of interest. Over the tropical Pacific, the cold tongue SST bias is a common model bias in many state-of-the-art models (e.g. Meehl et al., 2005; Lin, 2007). MLD bias is less well-constrained between models but tends to show shallow biases (e.g. Huang et al., 2014).

For the forecasts of different timescales, subseasonal forecast is a challenging forecasting time scale, which aims at connecting short-range and seasonal predictions by considering lead times from 1 week up to 2 months. The sources of subseasonal predictability include the MJO, soil moisture, snow cover and sea ice, mid-latitude weather regimes (e.g., NAO, PNA, Blocking), stratosphere-troposphere interactions, ocean conditions, and tropical–extratropical teleconnections (e.g. Vitart, 2017; Robertson and Vitart, 2019). Since predictability of tropical weather on subseasonal timescales can be influenced by ocean states and air-sea interaction (e.g. DeMott et al., 2015), understanding the upper ocean evolution and air-sea interaction processes over tropical Pacific is important for processes varying on subseasonal timescales.

Previous studies have shown that both the different data assimilation methods and different observational data availability in the tropical Pacific Ocean are important for ocean states and forecast (e.g. Fujii et al., 2015; Xue et al., 2017; Doblas-Reyes et al., 2011; Carrassi et al., 2016). The impact of the ocean data assimilation on subseasonal forecast is less well-understood. Therefore, this study aims to understand how data assimilation of in-situ ocean observation can influence the ocean's initial states in the coupled forecast model and the subseasonal forecasts of SST and MLD.

In this study, we examine tropical Pacific ocean forecast of the SST and MLD using the European Centre for Medium-Range Weather Forecasts (ECMWF) coupled model forecasts initialized with different ocean states that were produced by assimilating or not assimilating in-situ ocean observations, which are called Observing System Experiments (OSEs) (Zuo et al., 2019). The model information, experimental designs, and error calculations are described in Section 2. In Section 3, the differences between the two OSE analyses (i.e., the initial condition of the subseasonal forecasts) and their errors are first examined and discussed. Next, we show how the SST and MLD evolve differently between the two OSEs and how their forecast errors evolve in these OSE subseasonal forecasts. The physical mechanisms that lead to the SST difference and the roles of initialization shock and model biases that lead to the MLD jump are also discussed. As described in the final section, we conclude that assimilating in-situ observations leads to smaller SST errors, but the benefits are diminished by MLD biases and initialization shock, and that air-sea coupling and subsurface processes are the main drivers of differences in subseasonal SST forecasts with and without ocean data assimilation.

2 | MODEL AND METHODOLOGY

2.1 | ECMWF ORAS5 reanalysis

The ocean and sea-ice reanalyses are generated by using an ocean–sea-ice coupled model driven by atmospheric surface forcing and constrained by ocean observations via a data assimilation method (Balmaseda et al., 2015). These reanalysis products provide reconstructions of the ocean and sea-ice states, which are considered to represent observational states in some of the analyses. The OCEAN5 system is the fifth generation of the operational ocean ensemble reanalysis–analysis system at ECMWF. The OCEAN5 historical reconstruction of the ocean and sea-ice state is the ORAS5 reanalysis, which includes five ensemble members and covers the period 1979 onwards, with a back extension to 1958 (Zuo et al., 2019). The ocean model used for ORAS5 is the NEMO ocean model version 3.4.1 (Madec

and the NEMO team (2008), plus specific modifications implemented at ECMWF, as reported by Zuo et al. (2019) and references therein; Vidard et al. (2015)). The model horizontal resolution is approximately 25 km in the tropics and increases to 9 km in the Arctic (ORCA0.25, Bernard et al. (2006); Madec and Imbard (1996)). The vertical level spacing increases from 1 m at the surface to 200 m in the deep ocean with 75 vertical levels. The NEMOVAR (3D-VAR) is used to assimilate subsurface temperature, salinity, sea-ice concentration, and sea-level anomalies (SLA) with a 5-day assimilation window.

The in-situ temperature and salinity (T/S) profiles used in the data assimilation processes of the ORAS5 come from the EN4 data set (Good et al., 2013), which is a reprocessed observational dataset with globally quality-controlled ocean T/S profiles. This dataset includes all conventional oceanic observations (i.e., Argo, expendable bathythermograph (XBT) and mechanical bathythermograph (MBT), conductivity–temperature–depth (CTD), moored buoys, and ship and mammal-based measurements).

2.2 | ECMWF OSE reanalyses and subseasonal forecasts

Observing system experiment (OSE) is a method of evaluating the impact of existing observations on ocean states or forecasts. The OSE reanalyses are generated with a similar process of generating reanalysis product but modifying how much data we use during the data assimilation process (e.g. Fujii et al., 2015; Balmaseda and Anderson, 2009). By comparing ocean states of the OSEs reanalyses or forecasts initialized with different assimilated data products, we can evaluate the impact of observational data.

The OSE reanalyses at ECMWF are performed with the Ocean Reanalysis Pilot 5 (ORAP5)-equivalent low-resolution configuration at ORCA1.L42 resolution (approximately 1° at tropics with 42 vertical levels, Madec and Imbard (1996); Balmaseda et al. (2013)) with the bias correction and SLA assimilation switched off (i.e., a similar process as generating ORAS5 but with modified settings and lower resolution). The atmospheric forcing of these OSE reanalyses is from ERA-Interim. All these OSE reanalyses use strong SST constraints by nudging the SST to HadISST2 before 2008 and OSTIA operational analysis after 2008. A reference experiment is performed by assimilating all of the in-situ subsurface ocean observations into the ocean model to generate the AllObs OSE ocean reanalysis. Another OSE reanalysis (named NoInsitu) was carried out by withdrawing all of the in-situ observations from the global data assimilation system, which is only constrained by atmospheric reanalyses surface fluxes and SST. Comparing these two OSE reanalyses can help us evaluate the impact of the Global Ocean Observing System (GOOS) on subseasonal forecasts.

In order to understand how different observational data influence the forecast, these OSE reanalyses data are used as the initial conditions of the subseasonal reforecasts (called forecasts hereafter) in the ECMWF Integrated Forecasting System (IFS). These coupled subseasonal forecasts based on the different OSE reanalyses as the initial condition are integrated for 32 days starting from the first day of each month between 1993 to 2015 with a recent model cycle 47R1 of the ECMWF IFS. The atmosphere horizontal resolution of the IFS coupled forecast model is around 36 km with 91 vertical levels (TCo319/L91). The ocean horizontal resolution of the IFS coupled forecast model is approximately 1◦ at tropics with 42 vertical levels (ORCA1.L42). This resolution is the same as the model generating OSE reanalyses, which are used as the initial conditions of the forecast. Five ensemble members are generated in these OSE subseasonal forecasts corresponding to the five ensemble members in the ORAS5.

In these OSE reanalyses, SST relaxation/nudging is performed in both the AllObs and NoInsitu experiments, reducing the difference between the AllObs and NoInsitu experiments caused by the difference in ocean data assimilation. This SST relaxation process also means that the direct difference in the data assimilation between AllObs and NoInsitu is mainly within the subsurface ocean. We use the shortened name AllObs and NoInsitu to emphasize the main difference in the data assimilation process between the two experiments. However, the subsurface ocean difference

(e.g., MLD) between the two OSEs is from the direct impact of data assimilation, while the SST difference is indirect.

2.3 | Model forecast error calculation

While analyzing these OSE subseasonal forecasts, we calculate the ocean forecast error by comparing the forecasts with the ORAS5 ocean reanalyses data, which can be considered as a reference state that roughly represents observational states. The reanalysis synthesizes available observations with model physics to generate ocean state estimates that are resolved in space and time. The ORAS5 SST was shown to have warm biases in the eastern equatorial Pacific and cold biases near the warm pool when compared to satellite observation (i.e., ESA SST CCI Version 1.1 (Merchant et al., 2016)) (Zuo et al., 2019). The forecast errors, therefore, are different if other ocean reanalyses are used as the reference because different ocean reanalyses can produce different estimates of historical ocean states. Since the same ocean model was used to generate the ORAS5 reanalysis and the OSEs, using ORAS5 reanalysis as the reference gives us smaller forecast errors. The forecast errors calculated in this study are mainly used to provide a forecast error pattern that can help us understand and compare the two OSE subseasonal forecasts.

Forecast errors can be the result of model drift toward climatological states caused by the model physics, resolution, and parameterization, but also other error sources caused by different forcings and initial conditions (e.g., data assimilation methods, data availability, and other initialization processes). The initial errors of the model forecast (i.e., OSEs−ORAS5) are due to the difference between OSEs and ORAS5 model setup (e.g., OSEs are generated with lower resolution, no SLA assimilation, and no bias correction, compared to ORAS5) and the data availability (only for NoInsitu, with no ocean in-situ data assimilation). These errors in the ocean's initial conditions will interact with the model drift toward the climatological model bias. Depending on the modeled variable, evidence of model drift toward its preferred climatological state can be observed within the first few days of the forecast, and can therefore affect subseasonal forecasts, as discussed further in Section 3.2.2. It is worth noting that because the OSE reanalyses used a similar methodology and model as the ORAS5, by using ORAS5 as the reference of forecast error, OSEs (especially AllObs) can result in smaller forecast errors.

As for comparing the two OSE experiments, the designed difference is due to different data availability in the assimilation processes. On the other hand, the atmospheric states are identical at the initial time of the two OSE subseasonal forecasts although they can evolve differently later in the forecast through coupled processes.

3 | RESULTS

3.1 | Analysis of OSE forecast initial conditions

The initial conditions of these OSE subseasonal forecasts are the OSE reanalysis generated with different observing system data assimilated. Therefore, the difference between the initial conditions of these two OSE subseasonal forecasts represents how assimilating ocean in-situ observations influences the ocean states.

The SST initial condition of the subseasonal forecast shows cold errors for both AllObs and NoInsitu experiments over the equatorial central to eastern Pacific, compared to ORAS5 (Fig. 1a,b). These initial cold errors in the AllObs experiment are weaker than those in the NoInsitu experiments meaning that assimilating the in-situ ocean observation helps bring the SST toward the ORAS5 ocean reanalysis data. Notice that because the ECMWF OSEs and ORAS5 use the same ECMWF OCEAN5 system, the difference between the OSE AllObs and ORAS5 comes from the difference in model setup, which includes the lack of SLA assimilation and bias correction and the lower resolution in the OSE experiments (Zuo et al., 2019). The initial SST difference (i.e., AllObs−NoInsitu, Fig. 1c) over the tropical Pacific shows

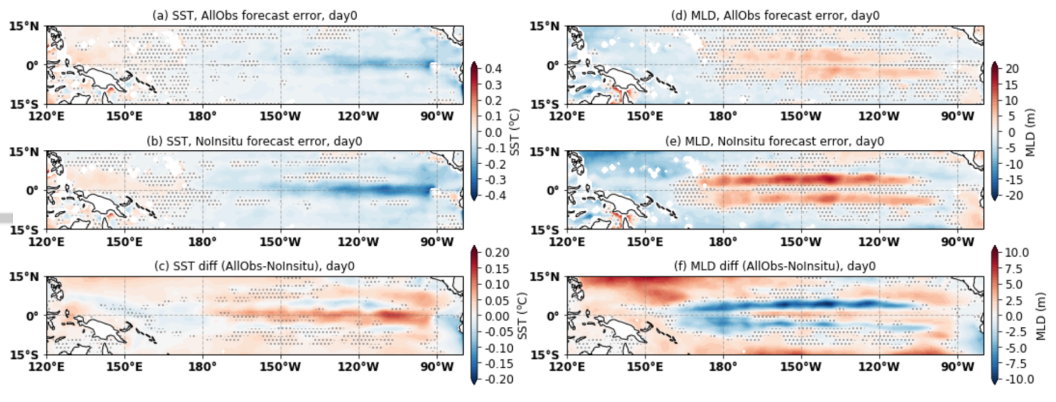

FIGURE 1 The SST (°C) errors (OSE−ORAS5) of (a) AllObs and (b) NoInsitu and (c) the difference between the AllObs and NoInsitu experiment at the initial time (day 0), which is also the difference between AllObs forecast error and NoInsitu forecast error because the errors are calculated with the same reference, ORAS5. (d,e,f) Same as (a,c) but for MLD (m). Stippling indicates two OSE experiments are NOT significantly different at the 95% significance level. These results are averaged of all the forecasts from 1993 to 2015 with 5 ensemble members. Notice that these initial conditions of the OSE forecasts are the OSE reanalyses.

a pattern of warm difference (i.e., assimilating the in-situ ocean observations results in warmer SST) in the equatorial central to eastern Pacific and cold difference in the equatorial western Pacific and the east of Galapagos Islands (approximately at 90°W). Both initializations have cold errors over the cold tongue region when the ORAS5 is used as the reference state, but the error is smaller in AllObs than in NoInsitu.

The subsurface ocean density structure, which can be characterized by MLD, is important for SST evolution since it controls the amount of SST increase per unit heat input. The ocean MLD output used in this study is defined by the depth that sigma-theta (the density calculated with in-situ salinity and potential temperature and with pressure equal to zero, minus 1000 kg m^{-3}) has increased by 0.01 kg m^{-3} relative to the near-surface value at 10 m depth. At the initial time of the forecast, the MLD near the equatorial Pacific has deep errors compared to the ORAS5, and the errors in AllObs experiment are weaker compared to the NoInsitu experiment (Fig. 1d,e). The weaker errors in AllObs experiment imply that assimilating ocean in-situ observations reduces the deep MLD errors.

A strong shallow MLD difference shows up in the central Pacific and extends eastward to around 105°W at each side of the equator (Fig. 1f). On the other hand, from near the eastern edge of the western Pacific warm pool to the eastern Pacific, a region of deep MLD difference is located exactly along the equator. These lead to a tripolar pattern of the MLD difference in the meridional direction over the deep tropics.

The SST differences between the two initial conditions have a clear spatial structure reminiscent of the ocean model errors. For instance, over the equatorial central to eastern Pacific, where the SST is too cold, the assimilation increment is warming the SST in the initial condition of AllObs experiment while no assimilation increment is applied on the initial condition of the NoInsitu experiment (i.e., the warm difference between AllObs and NoInsitu). The SST relaxation, on the other hand, reduces the warm difference between AllObs and NoInsitu by adjusting the NoInsitu toward higher SST, with a larger magnitude compared to the SST relaxation adjustment in AllObs experiment. Although the difference in SST caused by data assimilation is reduced partly by the SST relaxation, the net effect in this region follows the assimilation increment. In other words, over the equatorial central to eastern Pacific, where the model

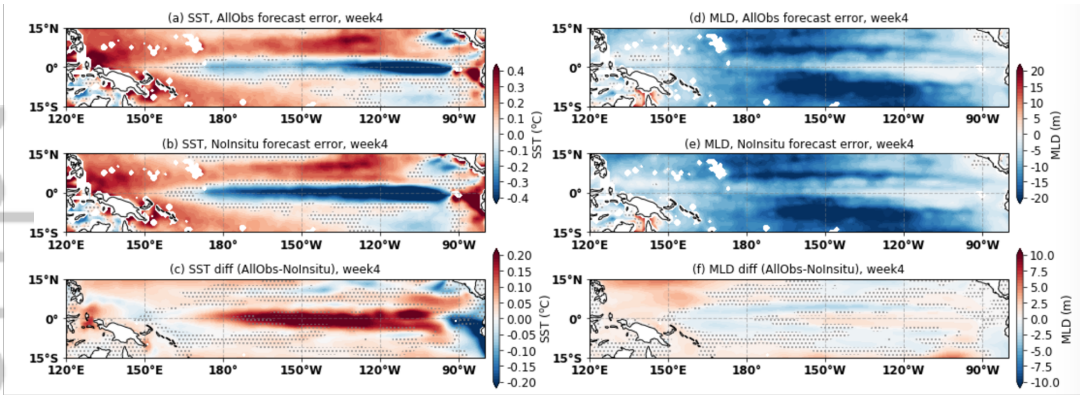

FIGURE 2 Same as Fig. 1 but for week 4.

tends to produce a colder SST compared to ORAS5, even with the SST relaxation, the assimilation of in-situ ocean observations would lead to warm SST difference between AllObs and NoInsitu experiments.

Another feature over the equatorial Pacific is the dipole structure of the SST difference across the Galapagos Islands (Fig. 1c). Previous studies show that missing proper representation of the Galapagos Islands across the equator in the model would lead to warm biases to the west of the islands and cold biases to the east of the Islands (e.g. Karnauskas et al., 2007). This is because the model does not capture the cold pool to the west of the islands due to the lack of blocking effect of the equatorial undercurrent. Although the OSE subseasonal reanalysis has only approximately 1-degree horizontal resolution, which cannot capture the Galapagos Islands at the equator well, with the effects of the data assimilation and SST relaxation in the reanalysis data, the local cold pool structure to the west of the Island exists (not shown). The dipole pattern of SST biases (warm to the west of the Island and cold to the east) due to the lack of well-represented islands in the model output is therefore not seen. Instead, the equatorial eastern Pacific west of the island is dominated by the cold errors (Fig. 1a,b). Mechanisms explaining the SST evolution across the Galapagos Islands are discussed in the next section.

3.2 | Evolution of OSE subseasonal forecast errors and differences

After identifying the different initial conditions in these OSE subseasonal forecasts due to ocean data assimilation, we are interested in examining how the SST and MLD in these forecasts can evolve differently. In general, the initial SST difference grows throughout the forecast, while the initial MLD difference weakens in the forecast with the patterns and signs remaining the same (Fig. 1c,f and 2c,f). The details of the SST and MLD evolution will be described in the following subsections respectively.

3.2.1 | Sea surface temperature

The pattern of the SST difference grows significantly in the subseasonal forecast over the equatorial central to eastern Pacific and the east of Galapagos Islands (Fig. 2c). At week 4, the SST cold errors over the central to eastern equatorial Pacific grow in both OSE subseasonal forecast experiments while the AllObs experiment still has weaker forecast

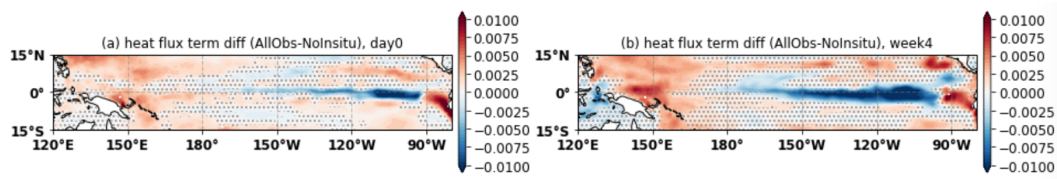

FIGURE 3 The mixed layer temperature tendency (°C d^{-1}) due to heat fluxes term at the (a) initial time and (b) week 4. Positive values indicate warming the ocean mixed layer. Stippling indicates two OSE subseasonal forecast experiments are NOT significantly different at the 95% significance level.

errors compared to the NoInsitu experiment (Fig. 2a,b). This implies that for the SST, the small initial difference in the tropical Pacific due to ocean data assimilation could evolve into a large SST forecast difference and reduce the SST errors in the forecast.

To examine why the SST difference between the AllObs and NoInsitu grows in the forecast, the mixed layer temperature budget is considered. Based on the mixed layer temperature budget (e.g. Stevenson and Niiler, 1983; Li et al., 2016), the mixed layer temperature (i.e., approximately SST) tendency ($\partial SST/\partial t$) can be changed by the surface heat flux terms (the solar radiation (SW_{sfc}), longwave radiation (LW_{sfc}), sensible heat (SH), and latent heat fluxes (LH) at the surface, and penetration of solar radiation at the bottom of mixed layer depth (SW_{MLD}) (i.e., surface heat flux term = $SW_{sfc} + LW_{sfc} + SH + LH - SW_{MLD}$) and the ocean processes (e.g., horizontal advection, vertical advection and entrainment).

The OSE forecast does not contain all the variables required for the mixed layer temperature budget. However, we have computed the surface heat flux contributions and used the residual to represent the ocean processes in our analysis. The penetration of the solar radiation of the OSE forecasts is calculated according to a two-waveband light penetration scheme ($I(z) = I(0)[\mathrm{R}e^{-z/\zeta_1} + (1-\mathrm{R})e^{-z/\zeta_2}]$, where the I($z'$) is the downward irradiance at depth z', R is the red light fraction, ζ_1 the penetration depth scale of red light, and ζ_2 the penetration depth scale of blue light) with a type I water classification (R = 0.58, ζ_1=0.35m, and ζ_2=23m) (e.g. Paulson and Simpson, 1977; Jerlov, 1976).

To understand the surface heat flux contribution to the SST difference evolution of the OSE subseasonal forecasts, we calculate the difference in the heat fluxes term between AllObs and NoInsitu experiments. The differences are negative (i.e., heat flux is cooling the SST more in the AllObs) over the equatorial central to eastern Pacific (Fig. 3), where the growth of the SST warm difference is large. This implies that the impact of the difference in heat fluxes is leading to a reduction of warm SST difference while the SST has a warm difference between the AllObs and NoInsitu experiments over this region and the warm difference is growing stronger with time in the forecast.

The contrasting results between the difference in heat flux term and SST evolution suggest that the difference in the heat fluxes term is not the main reason that leads to the growth of warm SST difference, and, thus, either ocean process and/or dynamical feedbacks contribute to the growth of warm SST difference between the OSE subseasonal forecasts. For the tropical region east of the Galapagos Island, the heat fluxes term has a positive difference, which can not explain the growth of cold SST difference as well. The growth of initial SST differences in this region is also attributable to either ocean processes and/or dynamical coupled feedbacks (e.g., via wind changes) (Fig. 3).

The ocean processes and dynamical feedbacks can include many different mechanisms. One of the possible mechanisms that can influence the SST evolution is through the feedback between the zonal SST gradient, pressure gradient force, and surface zonal wind. The initial equatorial SST difference between the AllObs and NoInsitu shows a local warm maximum near 100°W, which forms an eastward SST gradient difference to its west and a westward SST

gradient difference to its east (Fig. 4a). The difference in the SST gradient can correspond to the difference in zonal pressure gradient force in the atmosphere and lead to a difference in the zonal surface wind (e.g. Lindzen and Nigam, 1987). The difference in the equatorial zonal wind can further lead to changes in the SST through piling up the warm surface water downstream, which can reinforce the initial SST gradient and form positive feedback (Fig. 5a).

The difference in 10 m zonal wind (Fig. 4b) shows a consistent pattern to the proposed mechanism that has an eastward surface wind difference to the west of the local maximum of the SST difference, and westward surface wind difference to the east of the maximum. This is evidence that the positive feedback described here based on the relation between wind and SST gradient can contribute to the evolution of the SST difference pattern in the forecast. Notice that the other possible mechanism governing the response of surface wind to SST pattern is that higher SST corresponds to stronger atmospheric mixing and therefore stronger surface wind magnitude influenced by the wind in the free atmosphere (i.e., the prevailing trade wind in this region) (e.g. Wallace et al., 1989; Hayes et al., 1989). If this local response is the dominating mechanism, the difference in the wind would be westward (eastward) near (away from) 100°W. This wind pattern is not seen from the wind difference evolution (Fig. 4b), which suggests that the wind response to the SST is dominated by the SST gradient mechanism (e.g. Lindzen and Nigam, 1987).

Other than the positive feedback regarding SST pattern, the difference in the surface wind pattern can also influence the SST evolution through other processes. Since the prevailing zonal wind in this region is the westward trade wind, the eastward wind difference over the west of 100°W at the equator can lead to the weakening of the trade wind and thus weaker Ekman suction and weaker mixing in the subsurface ocean. Both the weaker Ekman suction and mixing can lead to warmer SST in this region (Fig. 5b), which is consistent with the increasing warm SST difference in this region (Fig. 4a). Notice that this SST response to surface wind can also partly contribute to the process of how the difference in zonal wind results in the difference in zonal SST gradient in the positive feedback we discussed earlier (left purple arrow in Fig. 5a which points from Δ *Zonal wind* to Δ *Zonal SST gradient*).

The edge of positive and negative zonal wind difference is not well-colocated with the local SST maximum (indicated by the green dashed line in Fig. 4) later in the forecast. This might be caused by the increasing SST difference to the west of the local SST maximum due to the response to the surface wind (Fig. 5b). This increasing SST changes the pattern of the SST gradient with time, leading to a more complicated relation between the SST gradient difference and the wind difference. These SST difference evolution features between the OSEs are more obvious when the averaged equatorial region is selected to a narrower latitudinal range (i.e., from 5°S–5°N to 1°S–1°N), which reinforces the argument that the equatorial processes are contributing to the SST difference evolution (not shown).

3.2.2 | Mixed layer depth

In contrast to the growth of SST difference, the significant MLD difference in the initial condition decays in the subseasonal forecast (Fig. 1f and Fig. 2f). This suggests that assimilating the in-situ ocean observations, especially the temperature and salinity profiles, can largely influence the states of subsurface ocean density structure. However, while the difference caused by data assimilation tends to remain the same signs in the forecast, the abrupt weakening of this difference near the beginning of the forecast (not shown) implies that the information gained at the initial condition due to ocean in-situ data assimilation is lost rapidly in the forecast.

While the initial MLD errors tend to be smaller in the AllObs experiment (Fig. 1d,e), these MLD errors jump from positive (i.e., deep errors) to negative (i.e., shallow errors) at the beginning of the forecast and remain negative and large for the rest of the forecast (Fig. 2d,e, Fig. 6a,b). During the times that the shallow MLD errors dominate, the MLD difference between the AllObs and NoInsitu is much smaller than the MLD forecast errors (Fig. 2d,e,f), which suggests the shallow MLD model biases dominate the MLD evolution in the subseasonal forecasts and the in-situ

ocean data assimilation does not have large impacts on the MLD subseasonal forecast.

To further identify the jump of the MLD in the subseasonal forecast, the MLD at the 0th and 1st day of the forecasts are shown and compared with the ORAS5 MLD (Fig. 6c). The largest jump happens in the equatorial central to eastern Pacific and peaks near 160°W. In the ORAS5, the equatorial MLD peak is about 44m for both the 0th and 1st day of the forecast. The equatorial MLD peak in the AllObs experiment jumps from around 47 m on the 0th day to 26 m on the 1st day of the forecast. The MLD peak in the NoInsitu on the 0th day (49 m) is slightly deeper than that in AllObs experiment (47 m) and further away from the MLD in the ORAS5 (44 m). It also jumps abruptly to around 28 m on the 1st day. Based on the results that the MLD remains with similar depth in both the AllObs and NoInsitu experiment after the first few days of the forecast (Fig. 6a,b), the shallow MLD errors in the subseasonal forecast are considered to be model biases that emerge in this forecast model. This result is also consistent with the shallow MLD annual mean bias in the ECMWF model (Roberts et al., 2018).

This initialization shock in the coupled subseasonal forecasts could arise for different reasons. One of the reasons could be that the ocean model used for the reanalysis is uncoupled and the CORE bulk fluxes are used to force the ocean model at the surface for reanalysis. Given that the observations are assimilated in the ocean and atmosphere in an uncoupled framework, they may not result in a consistent and balanced coupled state for initializing coupled climate forecasts. Hence, when the coupled forecasts are initialized from this state and use the bulk fluxes produced by the coupled forecast model to force the ocean model, they can result in imbalances and coupled feedbacks that result in such initialization shocks. In addition, the coupled forecast system has a wave model coupled to the atmospheric model at the bottom surface that can modulate the winds and wind-driven mixing in the upper ocean. This wave coupling is missing in the ocean reanalyses. Such inconsistencies between the coupled model and uncoupled reanalyses could lead to initial jumps in the coupled forecasts before it adjusts to their biased state. Quantifying the initialization shock due to the uncoupled reanalysis initialization is beyond the scope of this study.

These initial MLD jumps in both AllObs and NoInsitu experiments imply that the information gained at the initial conditions due to ocean data assimilation is lost rapidly in the forecast. The initialization of the forecast would lead to the initialization shock, and the model biases can dominate the features of the subsurface ocean structure in these ECMWF model forecasts.

4 | CONCLUSION AND DISCUSSION

Ocean in-situ data assimilation can influence initial and forecasted ocean states, especially the subsurface thermohaline structure, which cannot be observed remotely. OSE experiments are designed by withdrawing observational data during the data assimilation processes, so differences between the OSE experiments can reveal the importance of assimilating observational data. In this study, by comparing the OSE subseasonal forecasts generated by ECMWF (AllObs and NoInsitu), we aim to examine how assimilating ocean in-situ observation can influence the ocean states (i.e., the initial conditions) and the subseasonal forecasts.

The difference in SST between the AllObs and NoInsitu at the initial time of the forecast is relatively small but grows significantly later in the forecast. The most significant features of the growing SST differences are the warm difference over the central to eastern equatorial Pacific and the cold difference east of the Galapagos Islands. This difference corresponds to smaller cold errors over the central to eastern Pacific and smaller warm errors east of the Galapagos Islands in the AllObs, which suggests that assimilating subsurface ocean in-situ observation can improve SST forecasts at the subseasonal timescale.

By the ocean mixed layer heat budget, we know that SST differences can be attributed to heat flux terms and

ocean dynamical processes such as horizontal advection and vertical mixing. Here, it is shown that the surface heat flux term has the opposite contribution to the SST difference evolution over the central to eastern equatorial Pacific, which implies that ocean processes are more important for the growth of the SST differences.

The surface zonal wind difference between AllObs and NoInsitu is eastward to the west of the local SST maximum, and westward to east of the maximum. Therefore, two mechanisms related to air-sea coupling are proposed to explain the significant growth of SST differences near the equatorial Pacific. One of the mechanisms is positive feedback between the zonal SST gradient, pressure gradient force, and surface winds. More specifically, an initial eastward zonal SST gradient difference can be related to the development of the eastward pressure gradient force difference, contributing to eastward wind difference. The eastward wind difference can reinforce the initial zonal SST gradient difference via accumulating warm water downstream—hence positive feedback. This can help the growth of the initial SST difference. The other mechanism is the ocean's response to the differences in surface wind speed. The easterly trade winds near the equatorial region in AllObs are weaker over the region west of the local SST maximum. The slower speed of trade wind here can correspond to weaker Ekman suction at the equator and weaker mixing in the ocean, both of which correspond to reduced SST cooling, which can further contribute to the growth of warm SST differences between AllObs and NoInsitu in this region. The region east of the local SST maximum can be explained by the same mechanism but with opposite signs. These results suggest that ocean dynamical processes that are coupled to the atmosphere can be important for the SST evolution in the forecasts.

The evolution of the subsurface ocean structure can be important for the air-sea coupling and the forecast. The MLD representation, which is one of the metrics used to quantify the subsurface ocean structure, is shown to have a significant improvement in the initial condition of the subseasonal forecasts over the tropical Pacific when the ocean in-situ observational data are assimilated. This improvement, however, decays later in the forecast. As for the errors, while the initial MLD error is smaller in the AllObs than in the NoInsitu, these initial deep errors change to strong shallow errors later in the forecast. This initial shift happens on the first day of the forecast and could be related to the initialization shock and model biases. This also implies that the MLD information gained from the ocean data assimilation procedure at the initialization is lost rapidly in the forecast.

Reasons for the sudden change of sign ("jump") of MLD bias at the beginning of a forecast remain elusive. If the jump is due to model biases, then the forward model needs improvement with improved process understanding and representation—particularly its subsurface ocean simulation. If the jump is mainly due to assimilation shock, then the data assimilation methodology especially coupled data assimilation needs improvement to generate consistent coupled initial conditions that the model physics are adjusted to. Neither precludes the importance of in-situ data assimilation. Investigating the causes of MLD jump is beyond the scope of this study, and may be the subject of future studies using OSE subseasonal forecast experiments with the operational ocean resolution.

This study focuses only on the SST and MLD features which are more closely related to air-sea interaction processes. Other atmospheric and oceanic features can be also important and require further analysis. While this study utilized ECMWF OSE subseasonal forecasts, it is worth exploring OSE experiments on other subseasonal forecast models to determine the extent to which these results are a robust representation of systemic issues across models. The diagnosed processes that can lead to the development of the SST difference may be different, as well as the model bias and role of initialization shock. Also, while we calculated the forecast errors relative to the ORAS5 reanalysis, using other ocean reanalyses data or observational data may lead to slightly different results. This study however provides important information on the roles of ocean in-situ data assimilation in the SST and MLD over the tropical Pacific and how they can evolve differently in the subseasonal forecast through ocean dynamical processes and model biases.

Acknowledgements

This work was supported by the NOAA grant (NA18OAR4310405 and NA18OAR4310406) and the CIRES visiting fellowship. The OSE subseasonal forecasts are generated by ECMWF. The analyses were conducted on the CU Boulder Indopac computing cluster and NCAR Cheyenne cluster.

references

Balmaseda, M. and Anderson, D. (2009) Impact of initialization strategies and observations on seasonal forecast skill. *Geophysical Research Letters*, **36**. URL: https://agupubs.onlinelibrary.wiley.com/doi/abs/10.1029/2008GL035561.

Balmaseda, M., Hernandez, F., Storto, A., Palmer, M., Alves, O., Shi, L., Smith, G., Toyoda, T., Valdivieso, M., Barnier, B., Behringer, D., Boyer, T., Chang, Y.-S., Chepurin, G., Ferry, N., Forget, G., Fujii, Y., Good, S., Guinehut, S., Haines, K., Ishikawa, Y., Keeley, S., Köhl, A., Lee, T., Martin, M., Masina, S., Masuda, S., Meyssignac, B., Mogensen, K., Parent, L., Peterson, K., Tang, Y., Yin, Y., Vernieres, G., Wang, X., Waters, J., Wedd, R., Wang, O., Xue, Y., Chevallier, M., Lemieux, J.-F., Dupont, F., Kuragano, T., Kamachi, M., Awaji, T., Caltabiano, A., Wilmer-Becker, K. and Gaillard, F. (2015) The Ocean Reanalyses Intercomparison Project (ORA-IP). *Journal of Operational Oceanography*, **8**, s80–s97.

Balmaseda, M. A., Mogensen, K. and Weaver, A. T. (2013) Evaluation of the ecmwf ocean reanalysis system oras4. *Quarterly journal of the royal meteorological society*, **139**, 1132–1161.

Bernard, B., Madec, G., Penduff, T., Molines, J.-M., Treguier, A.-M., Le Sommer, J., Beckmann, A., Biastoch, A., Böning, C., Dengg, J. et al. (2006) Impact of partial steps and momentum advection schemes in a global ocean circulation model at eddy-permitting resolution. *Ocean dynamics*, **56**, 543–567.

Carrassi, A., Guemas, V., Doblas-Reyes, F., Volpi, D. and Asif, M. (2016) Sources of skill in near-term climate prediction: generating initial conditions. *Climate Dynamics*, **47**, 3693–3712.

DeMott, C. A., Klingaman, N. P. and Woolnough, S. J. (2015) Atmosphere-ocean coupled processes in the Madden-Julian oscillation. *Reviews of Geophysics*, **53**, 1099–1154.

Doblas-Reyes, F. J., Balmaseda, M. A., Weisheimer, A. and Palmer, T. N. (2011) Decadal climate prediction with the european centre for medium-range weather forecasts coupled forecast system: Impact of ocean observations. *Journal of Geophysical Research: Atmospheres*, **116**. URL: https://agupubs.onlinelibrary.wiley.com/doi/abs/10.1029/2010JD015394.

Fujii, Y., Cummings, J., Xue, Y., Schiller, A., Lee, T., Balmaseda, M. A., Rémy, E., Masuda, S., Brassington, G., Alves, O., Cornuelle, B., Martin, M., Oke, P., Smith, G. and Yang, X. (2015) Evaluation of the Tropical Pacific Observing System from the ocean data assimilation perspective. *Quarterly Journal of the Royal Meteorological Society*, **141**, 2481–2496.

Good, S. A., Martin, M. J. and Rayner, N. A. (2013) EN4: Quality controlled ocean temperature and salinity profiles and monthly objective analyses with uncertainty estimates. *Journal of Geophysical Research: Oceans*, **118**, 6704–6716.

Hayes, S. P., McPhaden, M. J. and Wallace, J. M. (1989) The Influence of Sea-Surface Temperature on Surface Wind in the Eastern Equatorial Pacific: Weekly to Monthly Variability. *Journal of Climate*, **2**, 1500–1506.

Huang, C. J., Qiao, F. and Dai, D. (2014) Evaluating CMIP5 simulations of mixed layer depth during summer. *Journal of Geophysical Research: Oceans*, **119**, 2568–2582.

Jerlov, N. (1976) Marine Optics. In *Elsevier Oceanography Series*, vol. 14, vii. Elsevier.

Karnauskas, K. B., Murtugudde, R. and Busalacchi, A. J. (2007) The Effect of the Galápagos Islands on the Equatorial Pacific Cold Tongue. *Journal of Physical Oceanography*, **37**, 1266–1281.

Li, Y., Han, W., Wang, W. and Ravichandran, M. (2016) Intraseasonal Variability of SST and Precipitation in the Arabian Sea during the Indian Summer Monsoon: Impact of Ocean Mixed Layer Depth. *Journal of Climate*, **29**, 7889–7910.

Lin, J.-L. (2007) The Double-ITCZ Problem in IPCC AR4 Coupled GCMs: Ocean–Atmosphere Feedback Analysis. *Journal of Climate*, **20**, 4497–4525.

Lindzen, R. S. and Nigam, S. (1987) On the Role of Sea Surface Temperature Gradients in Forcing Low-Level Winds and Convergence in the Tropics. *Journal of the Atmospheric Sciences*, **44**, 2418–2436.

Lukas, R. and Lindstrom, E. (1991) The mixed layer of the western equatorial Pacific Ocean. *Journal of Geophysical Research: Oceans*, **96**, 3343–3357.

Ma, H.-Y., Xie, S., Klein, S. A., Williams, K. D., Boyle, J. S., Bony, S., Douville, H., Fermepin, S., Medeiros, B., Tyteca, S., Watanabe, M. and Williamson, D. (2014) On the Correspondence between Mean Forecast Errors and Climate Errors in CMIP5 Models. *Journal of Climate*, **27**, 1781–1798.

Madec, G. and Imbard, M. (1996) A global ocean mesh to overcome the north pole singularity. *Climate Dynamics*, **12**, 381–388.

Madec, G. and the NEMO team (2008) NEMO ocean engine. *Note du Pôle de modélisation, Institut Pierre-Simon Laplace (IPSL), France*, **No 27**.

Maes, C., Picaut, J. and Belamari, S. (2002) Salinity barrier layer and onset of El Niño in a Pacific coupled model. *Geophysical Research Letters*, **29**, 59–1–59–4.

Meehl, G. A., Covey, C., McAvaney, B., Latif, M. and Stouffer, R. J. (2005) Overview of the coupled model intercomparison project. *Bulletin of the American Meteorological Society*, **86**, 89–93.

Merchant, C. J., Embury, O., Roberts-Jones, J., Fiedler, E. K., Bulgin, C. E., Corlett, G., Good, S., McLaren, A.and Rayner, N. and Donlon, C. (2016) Esa sea surface temperature climate change initiative (esa sst cci): Analysis long term product version 1.1. *Tech. Rep., Centre for Environmental Data Analysis*.

Paulson, C. A. and Simpson, J. J. (1977) Irradiance Measurements in the Upper Ocean. *Journal of Physical Oceanography*, **7**, 952–956.

Roberts, C. D., Senan, R., Molteni, F., Boussetta, S., Mayer, M. and Keeley, S. P. E. (2018) Climate model configurations of the ECMWF Integrated Forecasting System (ECMWF-IFS cycle 43r1) for HighResMIP. *Geoscientific Model Development*, **11**, 3681–3712.

Robertson, A. W. and Vitart, F. (2019) *Sub-seasonal to seasonal prediction: the gap between weather and climate forecasting*. Elsevier.

Shi, J., Tang, C., Liu, Q., Zhang, Y., Yang, H. and Li, C. (2022) Role of mixed layer depth in the location and development of the northeast pacific warm blobs. *Geophysical Research Letters*, **49**, e2022GL098849.

Sprintall, J. and Tomczak, M. (1992) Evidence of the barrier layer in the surface layer of the tropics. *Journal of Geophysical Research*, **97**, 7305.

Stevenson, J. W. and Niiler, P. P. (1983) Upper Ocean Heat Budget During the Hawaii-to-Tahiti Shuttle Experiment. *Journal of Physical Oceanography*, **13**, 1894–1907.

Vidard, A., Bouttier, P.-A. and Vigilant, F. (2015) NEMOTAM: tangent and adjoint models for the ocean modelling platform NEMO. *Geoscientific Model Development*, **8**, 1245–1257.

Vitart, F. (2017) Madden—Julian Oscillation prediction and teleconnections in the S2S database. *Quarterly Journal of the Royal Meteorological Society*, **143**, 2210–2220.

Wallace, J. M., Mitchell, T. P. and Deser, C. (1989) The Influence of Sea-Surface Temperature on Surface Wind in the Eastern Equatorial Pacific: Seasonal and Interannual Variability. *Journal of Climate*, **2**, 1492–1499.

Wei, H.-H., Subramanian, A. C., Karnauskas, K. B., DeMott, C. A., Mazloff, M. R. and Balmaseda, M. A. (2021) Tropical Pacific Air-Sea Interaction Processes and Biases in CESM2 and Their Relation to El Niño Development. *Journal of Geophysical Research: Oceans*, **126**, e2020JC016967.

Xue, Y., Wen, C., Kumar, A., Balmaseda, M., Fujii, Y., Alves, O., Martin, M., Yang, X., Vernieres, G., Desportes, C., Lee, T., Ascione, I., Gudgel, R. and Ishikawa, I. (2017) A real-time ocean reanalyses intercomparison project in the context of tropical pacific observing system and ENSO monitoring. *Climate Dynamics*, **49**, 3647–3672.

Zuo, H., Balmaseda, M., Tietsche, S., Mogensen, K. and Mayer, M. (2019) The ECMWF operational ensemble reanalysis–analysis system for ocean and sea ice: a description of the system and assessment. *Ocean Science*, **15**, 779–808.

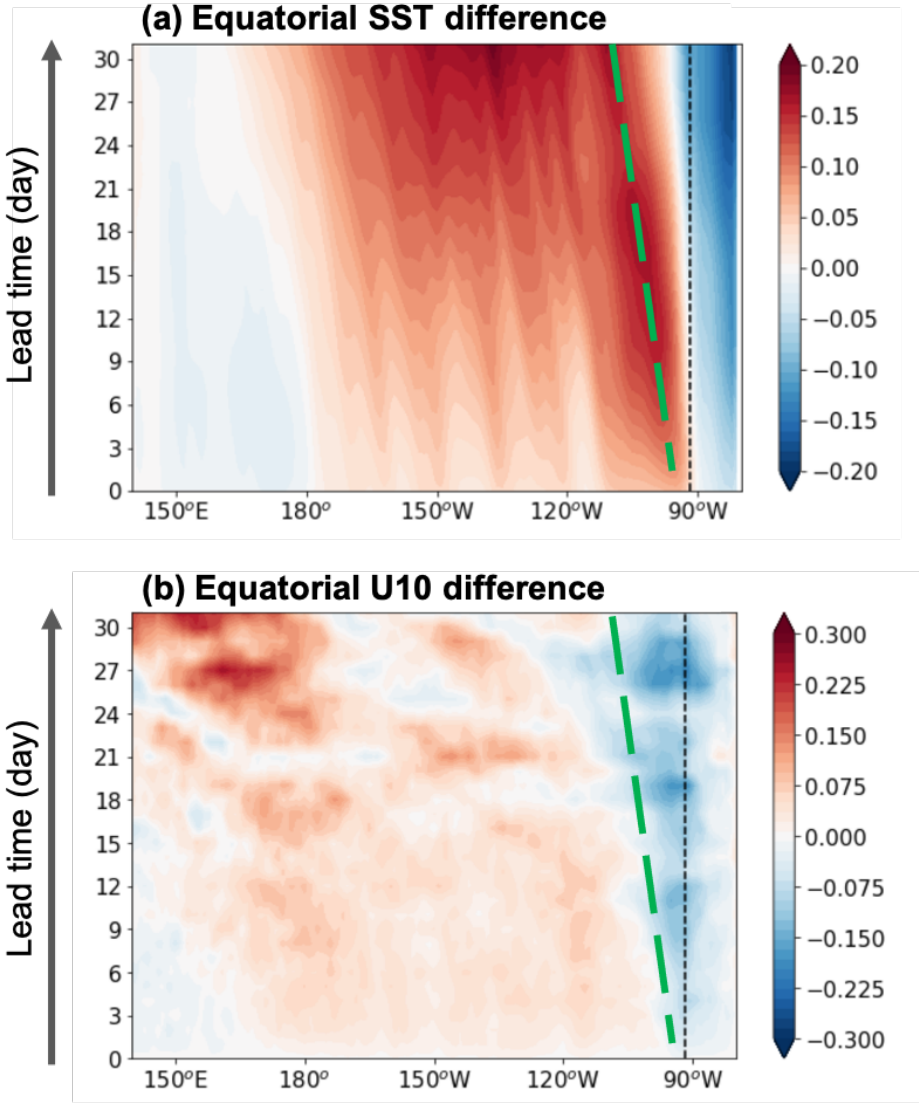

FIGURE 4 The evolution of equatorial (a) SST difference (°C) and (b) 10 meter zonal wind difference (m s^{-1}) between AllObs and NoInsitu averaged between 5°N and 5°S. The green dashed line indicates the evolution of the initial local SST maximum. The black dashed line indicates the western edge of the Galapagos Islands (91.7°W).

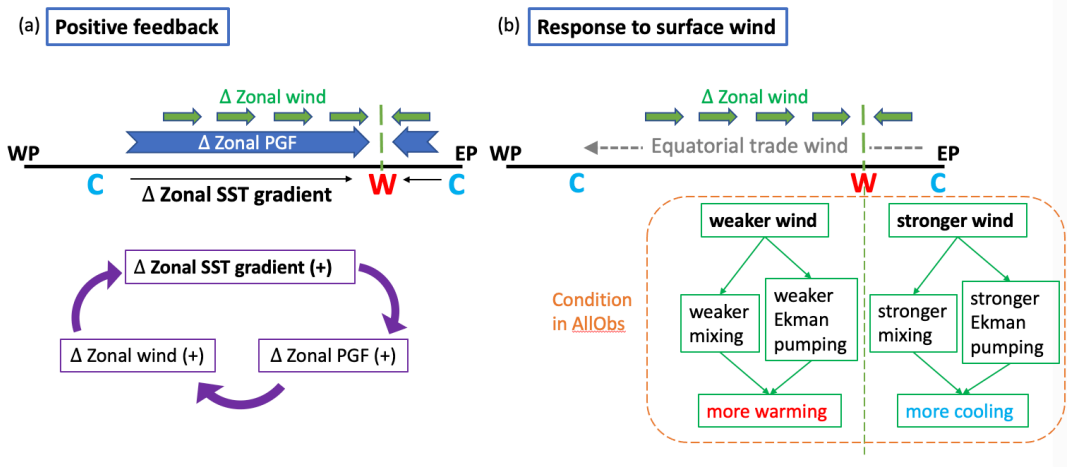

FIGURE 5 Schematic figures for the two mechanisms explaining the evolution of the SST difference. (a) The positive feedback between the zonal SST gradient, zonal pressure gradient force, and the zonal wind. (b) The different responses of SST to the surface wind magnitude.

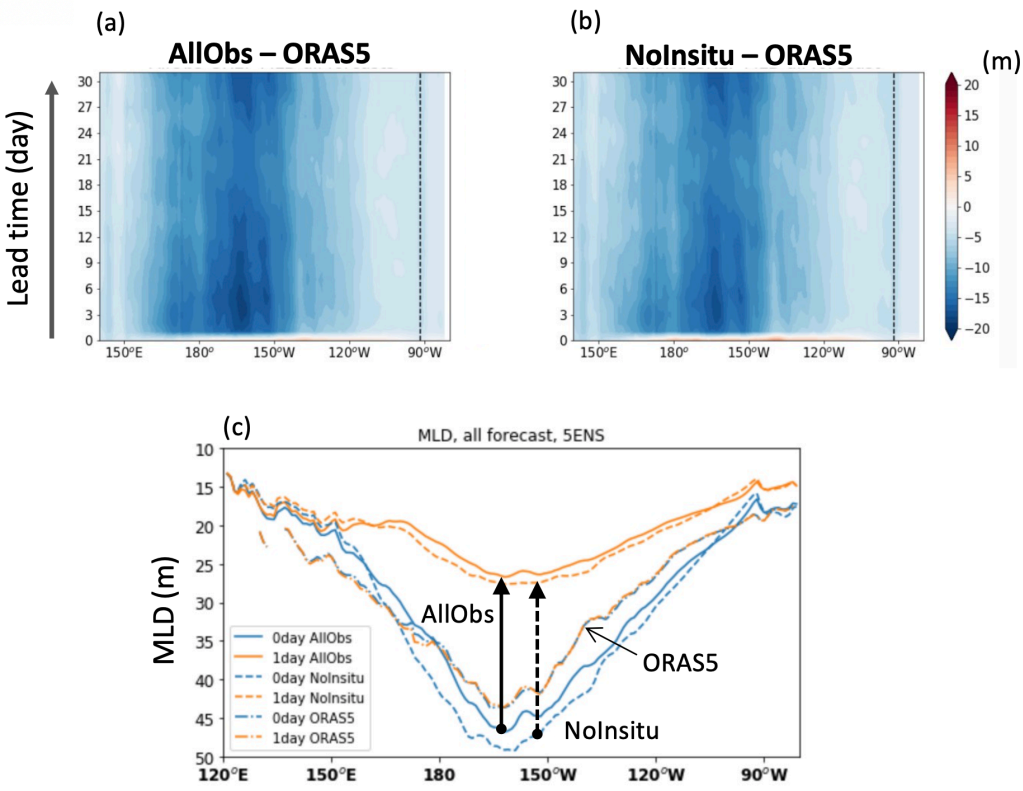

FIGURE 6 Evolution of the equatorial MLD bias (m) of (a) AllObs and (b) NoInsitu experiments averaged from 5°S to 5°N. (c) The MLD (m) averaged over all forecasts with 5 ensemble members at day 0 (blue) and day 1 (orange) in the AllObs (solid) and NoInsitu (dashed). The MLD in the ORAS5 reanalysis (dash-dotted) at the corresponding day 0 (blue) and day 1 (orange).